

OPTIMISATION OF LASER-FIRED ALUMINIUM EMITTERS FOR HIGH EFFICIENCY N-TYPE SI SOLAR CELLS

F. Granek, M. Hermle, B. Fleischhauer, A. Grohe, O. Schultz, S.W. Glunz, G. Willeke

Fraunhofer Institute for Solar Energy Systems, Heidenhofstr. 2, D-79110 Freiburg, Germany
Phone: +49-761-4588-5287; Fax: +49-761-4588-9250; email: filip.granek@ise.fraunhofer.de

ABSTRACT: In order to investigate the local laser-fired aluminium emitters (LFE), a process recently developed at Fraunhofer ISE, high-efficiency n^+np^+ back junction solar cells with resistivities of 1, 10 and 100 Ω cm were fabricated. The laser-induced damage was analysed and modelled using a two-dimensional DESSIS simulation. The injection-dependent Shockley-Read-Hall recombination in the direct vicinity of the local back-junction is believed to strongly influence the cell performance and cause large cell performance differences for different resistivity cells. Optimisation of the distance of laser-fired emitter points was performed. The importance of the annealing step following laser processing is shown. Effective excess carrier lifetimes of the 100 Ω cm FZ n -type Si up to 18 ms are reported.

Keywords: c-Si, High-Efficiency, n -type.

1 INTRODUCTION

The Laser-Fired Contact (LFC) technology developed at Fraunhofer ISE [1] not only provides local contacts through the dielectric passivation layer at the back cell side, but also creates a local aluminium doped regions. In case of p -type cells this region works as a high-low junction - an effective back surface field (BSF). This feature of the LFC process already enabled fabrication of a 21.9 % p -type solar cell. In addition to application of the LFC process to p -type substrates, an n -type substrate process with the use of the LFC has recently been introduced by Glunz et al. [2, 3]. The LFC process was used there to form local p - n back junctions on the n -type substrates, referred to as laser-fired aluminium emitter (LFE) process.

The LFE cell process, in which Al is laser-fired through the thermal oxide layer at the rear side, forming a local contact and alloying Al with Si in the n -type substrate, creates a local p^+ -emitter. Thus the fabrication of high efficiency n -type cells without the use of the high-temperature boron diffusion is possible. Moreover, the laser processing time stays in the range of seconds in comparison to hours of the boron diffusion, leading to considerable process cost reduction.

However, to realise high-efficiency cells using the back junction cell structure very thin substrates or high minority carrier diffusion lengths are required. The carriers most of which are generated near the front surface, need to travel through the whole cell thickness in order to be collected by the back-junction. n -type material, with its extremely high lifetimes (ms range already reported for multicrystalline silicon by Cuevas et al. [4]), is well suited for the fabrication of the back-junction cells.

An impressive efficiency of 19.4 % on 100 Ω cm FZ n -type material with the back junction LFE cells has already been demonstrated [2]. We believe however that the performance of these cells is still limited by the damage introduced by the laser process. In order to further improve the efficiency of cells with laser-fired aluminium emitters, a detailed analysis of the limiting factors of the LFE process is required. Thus gaining fundamental knowledge about the LFE process is the objective of this paper.

2 BACK JUNCTION N-TYPE SI SOLAR CELLS

2.1 LFE solar cell fabrication

n^+np^+ back junction cells (see Fig. 1) have been fabricated on 250 μ m thick FZ n -type 1, 10 and 100 Ω cm Si substrates. The size of the cells is 2x2 cm^2 . The cells exhibit a front surface with random pyramids, evaporated front contacts and a phosphorus diffusion ($\rho_{\text{sheet}} = 120 \Omega/\text{sq.}$) passivated by a 105 nm thick thermal oxide. The rear surface is covered with the same thermal oxide and a 2 μ m thick aluminium layer. The back junction is created by local laser-firing of the aluminium through the oxide layer resulting in an p^+ emitter and contact coverage of about 5 %. The last processing step is the low-temperature (425 $^\circ\text{C}$) annealing.

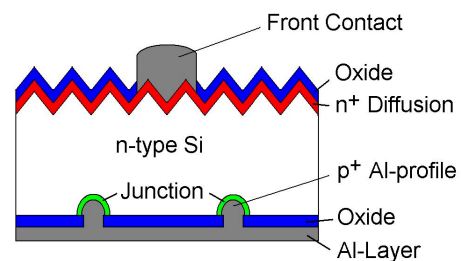


Figure 1: Structure of the n^+np^+ LFE cell.

2.2 Solar cells results

In Table I the most important results of different resistivity n -type LFE cells are summarised. Significant differences up to more than 20 % in j_{SC} of the 1, 10 and 100 Ω cm cells have been observed. Our first idea to explain this effect was to analyse diffusion length differences between these cells. The bulk lifetime and the holes mobility differences were analysed.

Table I. I-V results of the LFE cells fabricated on n -type FZ Si substrates with different resistivities.

Cell no.	ρ_{base} [Ω cm]	V_{oc} [mV]	j_{sc} [mA/cm^2]	FF	η [%]
NRP7_24.2m	100	646.5	39.8	0.751	19.4
NRP7_21.2m	10	639.8	37.9	0.719	17.4
NRP4_23.5	1	616.7	30.2	0.729	13.5

2.3 Bulk lifetime measurements

For the determination of the starting bulk lifetime of the used *n*-type material a few lifetime samples have been prepared. Both sides of these samples exhibit a full area shallow n^+ diffusion ($\rho_{\text{sheet}} = 120 \text{ } \Omega/\text{sq.}$) and a full area 105 nm thick thermal oxide.

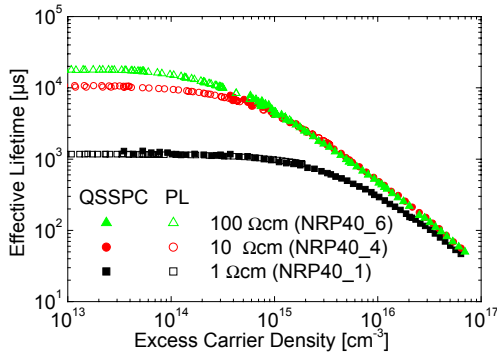


Figure 2: Injection-dependent bulk lifetime of FZ *n*-type Si wafers with different resistivity. Note that these are not fully processed solar cells, but only lifetime samples.

Extremely high effective lifetime (τ_{eff}) values – up to 18 ms - have been measured for the 100 Ω cm material (see Fig. 2) using quasi-steady-state photo-conductance (QSSPC) [5] and photoluminescence (PL) [6] measurement methods. This proves high lifetime of the *n*-type material.

Table II. Bulk lifetime and diffusion length for 1, 10 and 100 Ω cm *n*-type FZ Si.

Cell no.	ρ_{base} [Ω cm]	τ_{eff} [ms]	L_{eff} [μm]
NRP40_6	100	18.3	4710
NRP40_4	10	10.1	3492
NRP40_1	1	1.2	1175

The lifetime is high enough to realise perfect carrier collection by the back junction for all three resistivities. Even the 1 Ω cm material has the lifetime values above 1 ms resulting in a effective diffusion length (L_{eff}) of about 1200 μm which is more than 4 times the cell thickness. This leads to the conclusion that the bulk lifetime differences are not responsible for the large current differences between different resistivity cells.

3 LASER-INDUCED DAMAGE

3.1 Laser-induced damage zone

In previous work [2] a concept of a laser-induced damage zone (see Fig. 3) was introduced in order to explain V_{OC} as a function of doping concentration of the *p*-type LFC cells. Introduction of the damage zone with strongly reduced lifetime into the two-dimensional simulation model enabled very good modelling of the LFC *p*-type structures. The damage zone implemented in the simulation model had a size of 5 μm and strongly reduced lifetime of $\tau_{\text{local}} = 0.3 \text{ } \mu\text{s}$.

Since in case of the *n*-type cell the local Al-profile works as an emitter, the quality of this junction and the quality of the area in the direct vicinity of the junction is has a much bigger impact on the cell performance than in

the case of *p*-type cells, where the Al-profile works as a local back-surface-field (LBSF).

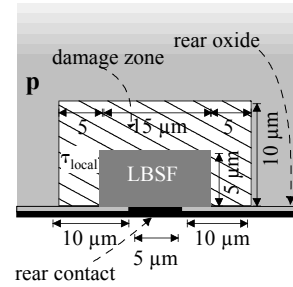


Figure 3: Two-dimensional simulation model of an LFC contact with a laser-induced damage zone of 5 μm around the local Al BSF.

3.2 Modelling of the internal quantum efficiencies

The internal quantum efficiencies (IQE) of the *n*-type LFE cells have been modelled using two-dimensional DESSIS [7] simulation. In the simulations an equal bulk lifetime $\tau_{\text{SRH}} = 1000 \text{ } \mu\text{s}$ was used for all three resistivities in order to investigate the influence of the damage zone separately. In Fig. 4 next to the IQEs of the LFE cells, the simulated IQEs are presented. The IQE of the cell with the damage zone model as well as the ideal case of a LFE cell without the damage zone have been modelled.

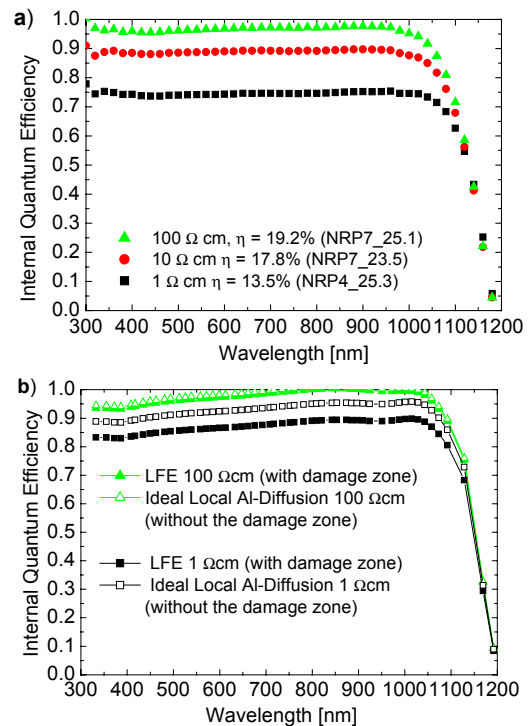


Figure 4: Measured (a) and two-dimensional DESSIS simulation (b) internal quantum efficiencies for the *n*-type LFE cells of different doping concentration.

The damage zone model enables modelling which is in a good agreement with the measured IQEs. We believe that the fine tuning of the damage zone parameters such as the size and lifetime, may result in even better agreement with the measured values.

One can see that the influence of the damage zone is much bigger for the 1 Ω cm material than in the case of 100 Ω cm, where the damage zone has almost no

influence on the quantum efficiency. The next section deals with the explanation of this effect.

3.3 Shockley-Read-Hall recombination in damage zone

Using the damage zone model the recombination rate and the density of the electrons and holes in the direct vicinity of the rear local junction have been simulated in two dimensions. In the Fig. 5 the recombination rate profile through the cell thickness is taken at the contact point.

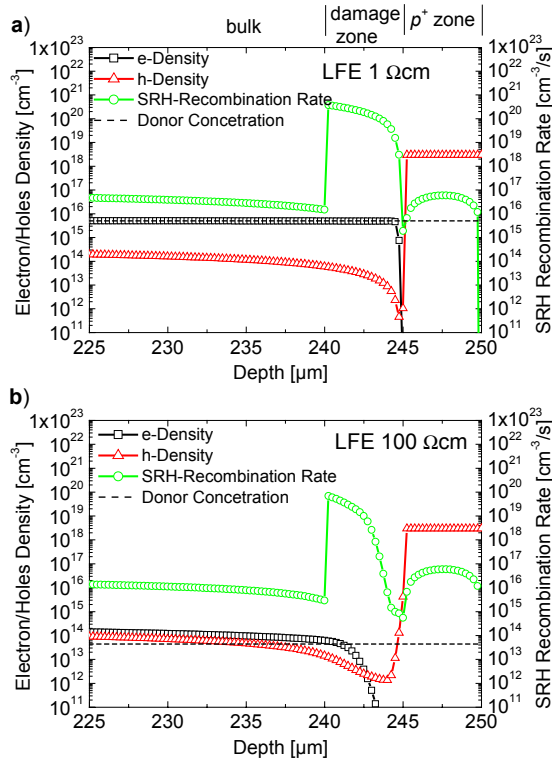


Figure 5: Profiles of the recombination rate under j_{sc} conditions of the 1 Ω cm (a) and 100 Ω cm (b) LFE cells taken through the cell thickness at the back surface of the cell (two-dimensional DESSIS simulation). Note the high recombination rate in the laser-induced damage zone (between 240-245 μ m from the cells front surface).

Shockley-Read-Hall (SRH) carrier lifetime is a function of the carrier injection level and the dopant density. In case of the 1 Ω cm material, where the injection level is lower than the dopant density (see Fig. 5 a), low injection level condition occurs ($\tau_{SRH, li}$). The dopant density of the 100 Ω cm material is however lower than the injection level (Fig. 5 b), thus the cell is under high injection ($\tau_{SRH, hi}$). Using the simplified SRH lifetime models under low- and high-level injection [8] and for $\tau_{no} = \tau_{po}$ the low- and high-level injection lifetime in *n-type* Si is:

$$\tau_{SRH, li} = \tau_{po} \text{ and } \tau_{SRH, hi} = \tau_{no} + \tau_{po}$$

Thus both bulk and damage zone lifetime of cells under high-injection is significantly higher than under low injection. We believe that this significant lifetime difference, resulting in a drastic change of the diffusion length in damage zone to the width of damage zone ratio,

is the reason of the performance difference between the LFE cells processed on the 1 and 100 Ω cm *n-type* wafers. Results of the simulation prove our hypothesis to be correct. The increased SRH recombination rate inside of the laser-induced damage zone around the LBSF area can be clearly seen. Furthermore, one can also see that the recombination rate of the 1 Ω cm cell in the bulk and inside the damage zone is almost one order of magnitude higher than in the case of 100 Ω cm, leading to a significant current decrease in the 1 Ω cm cells.

3.4 Suns V_{OC} measurements of the LFE cells

The Suns V_{OC} curves of the fully processed LFE cells have been measured in a wide light intensity range (Fig. 6) in order to analyse the cell performance under low- and high-injection level conditions.

The implied voltage of the starting material (lifetime samples described in section 2.3) has been calculated from the QSSPC lifetime curves as proposed by Sinton in [9] and plotted in Fig. 6 as well. For all the resistivities shape and values of the implied voltage are roughly the same in the range of 700 mV at one sun light intensity. These V_{OC} values represent an ideal state, where only bulk recombination (which is low for the good quality *n-type* material as shown before) and the low surface recombination rate play a role.

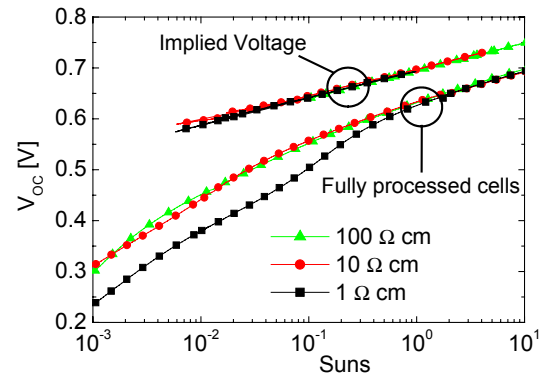


Figure 6: Open-circuit voltage and implied voltage in the wide light intensity range for different resistivity *n-type* lifetime samples and fully processed LFE cells respectively.

In the case of the fully processed LFE cells the Suns V_{OC} curves are different. First of all voltage values are lower. This is attributed to the cell structure where additional recombination mechanisms such as front and rear side metal contacts, laser-induced damage zone and texturization are introduced. All these elements reduce the voltage to 610-630 mV at one sun.

Additionally one can see an interesting shape of the 1 Ω cm curve of the LFE cell. Under low-injection intensities (light intensities < 0.3 Suns) the voltage decreases faster than in the case of higher resistivity cells. We believe that this is caused by a strong decrease in lifetime in the laser damage zone, where under low-injection the SRH recombination dominates – as discussed above.

One would expect a larger j_{sc} vs. Suns than a V_{OC} vs. Suns dependence, because under short-circuit conditions the cells operate at much lower injection levels as compared to open-circuit conditions. That is why the differences in j_{sc} are much more significant than the V_{OC} differences between 100, 10 and 1 Ω cm cells (Table I).

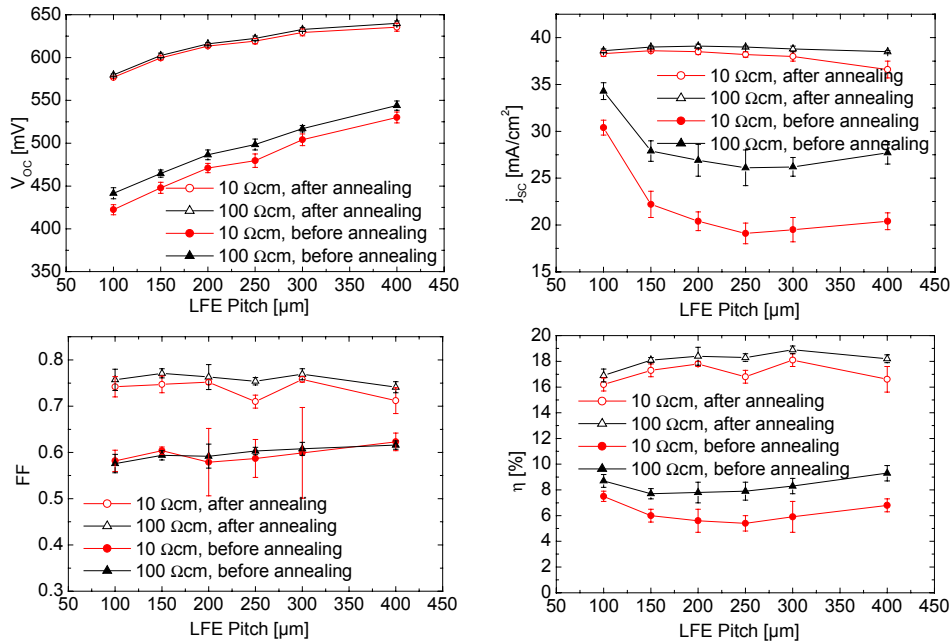


Figure 7: Results of the LFE cells processed with different pitch of the LFE process. Cell results both before and after annealing step are shown. Each data point represents the average of 7-16 cells. Spread in the results is also plotted on the graphs.

4 OPTIMIZATION OF LFE CELLS

In order to find the optimum between the emitter coverage, which should be large for efficient carrier collection at the back-junction and the damage introduced by laser, which should be as small as possible to reduce degradation of the cell performance, an optimisation of the pitch of the LFE points was performed. We chose the pitch range between 100 μm which allows a realisation of an almost full area emitter on the rear side (each LFE point is of about 70 μm diameter) and 400 μm which we expected to be already too much for a good carrier collection at the back side. Results are shown in Fig. 7.

As expected voltage improves with increasing pitch, because less damage is introduced by the laser. Current decreases very slowly with increasing pitch, because of the increase of the effective diffusion length which is required for the carriers to reach the local back junction. Fill factor is not affected by the pitch in the respective pitch range. The best efficiency of 19.4 % on the 100 Ω cm was realised for a pitch of 300 μm.

Both voltage and current of the 100 Ω cm is only slightly better than 10 Ω cm cells as both cell groups operate under medium- to high-injection. The importance of low-temperature (425 °C) annealing to achieve good cell results is also clear as it improves voltage, current and fill factor drastically.

5 CONCLUSIONS

Injection-dependent SRH recombination in the laser-induced damage zone is decisive to the LFE cell performance. Moreover it leads to strong performance differences between cells on different resistivity substrates. Extremely high bulk lifetime of 18 ms is

reported for 100 Ω cm *n*-type FZ Si wafer. Such high lifetime value enables fabrication of high-efficiency back-junction LFE cells with 19.4 % already reported. A low-temperature annealing step following the laser formation of the *p*-*n* junction is crucial to achieve good cell results.

ACKNOWLEDGEMENTS

The authors would like to thank S. Seitz, T. Leimenstoll, P. Richter and A. Herbolzheimer for processing as well as T. Roth for lifetime measurements and E. Schäffer for solar cell measurements.

REFERENCES

- [1] E. Schneiderlöchner, R. Preu, R. Lüdemann and S. W. Glunz, Prog. Photovolt. **10** (2002) 29-34.
- [2] S. W. Glunz, E. Schneiderlöchner, D. Kray, A. Grohe, M. Hermle, H. Krampwerth, R. Preu, G. Willeke, Proc. 19th EU-PVSEC, Paris, France (2004) 408-411.
- [3] S. W. Glunz, A. Grohe, M. Hermle, E. Schneiderlöchner, J. Dicker, R. Preu, H. Mäkel, D. MacDonald and A. Cuevas, Proc. 3rd WCPEC, Osaka, Japan (2003) 1332-1335.
- [4] A. Cuevas, M. J. Kerr, C. Samundsett, F. Ferazza and G. Coletti, Appl. Phys. Lett. **81** (2002) 4952-4954.
- [5] R. A. Sinton, A. Cuevas and M. Stuckings, Proc. 25th IEEE PVSC, Washington DC, USA (1996) 457-460.
- [6] T. Trupke, R. A. Bardos, F. Hudert, P. Würfel, A. Wang, J. Zhao, and M. A. Green, Proc. 19th EU-PVSEC, Paris, France (2004) 758-761.
- [7] TCAD-DESSIS, 8.5 ed. (TCAD, Synopsys), www.synopsys.com, Manual 2004.
- [8] S. Rein, T. Rehl, W. Warta, and S. W. Glunz, J. Appl. Phys., **91**, (2002) 2059-2070.
- [9] R. A. Sinton and A. Cuevas, Proc. 16th EU-PVSEC, Glasgow, UK (2000) 1152-1155.